Electron Microscopic Images of Crystals Observed with 300kV Electron Microscope (Special Issue on Electron Microscopy)

AUTHOR(S):

Hashimoto, Hatsujiro; Tanaka, Kenzo; Kobayashi, Keinosuke; Suito, Eiji

Electron Microscopic Images of Crystals Observed with 300 kV Electron Microscope

Hatsujiro HASHIMOTO*, Kenzo TANAKA** Keinosuke KOBAYASHI*** and Eiji SUITO***

(Institute for Chemical Research, Kyoto University)

Received January 20, 1965

Resolution of the electron microscopic images of crystalline films with certain thickness is discussed and some of the features observed in electron micrographs of crystal films taken at 250～300 kV are illustrated.

1. INTRODUCTION

It is generally believed that it is quite advantageous to use high voltage electron microscope for observing the microstructures of thin metallic films in high resolution, in high visibility and in reduced specimen damage by electron beam.

Because of these expectations, a number of microscopes operating at voltages in excess of 200 kV have been constructed.[1-9]

Some authors studied the energy dependence of the parameters involved in the theory of image contrast in crystalline materials. Kohra and Watanabe[10] studied the energy dependence of the absorption of electron waves in MgO smoke crystals using 100 kV electron microscope. Hashimoto *et al.*[11] studied energy dependence of the extinction distance and transmissive power of electron waves for crystals using 100 kV and 300 kV electron microscopes. Kobayashi *et al.*[12] studied energy dependence of the damage to the polymer crystals induced by the electron bombardment in the range of 75～300 kV. Hashimoto[13] studied the energy dependence of the contrast in the images of dislocations.

Their observations showed that the improvements in contrast, in visibility in thick specimens and reduced specimen damage by electron beam coincided with the theoretical expectations[14] in certain thickness of the crystals and in certain objective aperture sizes.

Dupouy *et al.*[15] studied the energy dependence of extinction distance and transmissive power for electron waves in MgO crystal by their microscope[9] which are operated up to 1.5 MeV. Dupouy *et al.*[16] showed also that the correspondence between the selected area of the specimen and its diffraction pattern is improved by elevating the accelerating voltages of electrons.

Dupouy *et al.*[17] observed with their microscope the inner structures of the metallic specimens with relatively large thickness at the accelerating voltages of 1000～1500 kV and obtained very clear images of these structures.

* 橋本初次郎 Department of Physics, Kyoto Technical University.
** 田中憲三 Department of Physics, Kyoto University.
*** 小林恵之助，水渡英二

In the present paper, the authors will review the consideration shown before[18] on the theoretical resolution of thick crystalline film and show some of the electron micrographs of crystals taken at 250～300 kV.

2. RESOLUTION OF THE IMAGES OF THICK CRYSTALS

The plane-parallel electron waves become divergent as going into the crystal by the elastic and inelastic collision with atoms. Since the well-focused electron microscopic images are the projection to the image plane of the intensity distribution of electrons appearing at the bottom surface of the crystal, the structures near the top surface are projected as diffuse images. A point at the top surface is projected to the bottom surface as a diffuse disk with the diameter

$$\delta_d = n(n+1)\xi_i\theta_0 , \qquad (1)$$

where n is the numbers of scattering, θ_0 is the angular deviation of electrons due to single inelastic scattering, and ξ_i is the mean free path of electrons in inelastic scattering. Then $n\xi_i = Z$ and $n\theta_0 = \theta_n$ where θ_n is the semiangle of divergence of electrons passing through the crystal with the thickness Z as shown in Fig. 1. θ_n can be measured from

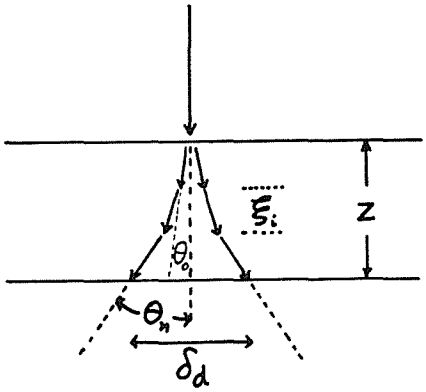

Fig. 1. Behavior of inelastically scattered electron in crystal. ξ_i, mean free path; δ_d, diameter of diffuse image of a point at the top surface.

the intensity distribution around the central spot in the diffraction pattern. Energy loss ΔE of the electrons passing through the crystal is approximately given by $n \cdot \Delta e$ where Δe is the loss due to a single scattering[19]. The errors of the electron microscopic images are chiefly due to the spherical and chromatic aberrations expressed by

$$\delta_s = C_s\alpha^3 , \qquad (2)$$

$$\delta_{chr} = C_{chr}(\Delta E/E)\alpha , \qquad (3)$$

where C_s and C_{chr} are spherical and chromatic aberration constants and α is the aperture of objective lens. The resolutions of the images[20] are given by

$$\delta_t = [(\delta_d)^2+(\delta_s)^2+(\delta_{chr})^2]^{1/2} \qquad (4)$$

for the structures near the top surface, and

$$\delta_b = [(\delta_s)^2+(\delta_{chr})^2]^{1/2} \qquad (5)$$

for the structures near the bottom surface.

Zworykin *et al.*[21] have made the detailed treatment on the resolution of the images of thick film. In the present treatment by assuming the values $\xi_i = 800$Å, $\theta_0 = 1.25\times10^{-4}$, $\Delta e = 10$ V, $\alpha = 5\times10^{-3}$, $C_s = C_{chr} = 0.3$ cm, and $E = 300$kV, δ_t and δ_b were calculated and are shown in Table 1. It can be seen in Table 1 that $2\sim4\,\mu$ are the maximum thickness of the general crystals whose structures can be detected in the same ambiguity.

Table 1. Resolution of images. Calculated values of δ_t and δ_b for scattering number n, divergence angle θ_n, and path length Z.

n	Z	$2\theta_n$	δ_t	δ_b
1	800 Å	2.5×10^{-4}	6.2 Å	6.2 Å
20	1.5 μ	5×10^{-3}	107 Å	100 Å
40	3.2 μ	1×10^{-2}	250 Å	195 Å
120	10 μ	3×10^{-2}	1520 Å	600 Å
200	16 μ	5×10^{-2}	4010 Å	990 Å

In order to see the difference of δ_t and δ_b, experimentally ZnO smokes were deposited on one side of the MoS_2 film of thickness 3μ[22] and electron microscopic images were photographed at 250kV by setting the film in the two ways so that the smokes are on top

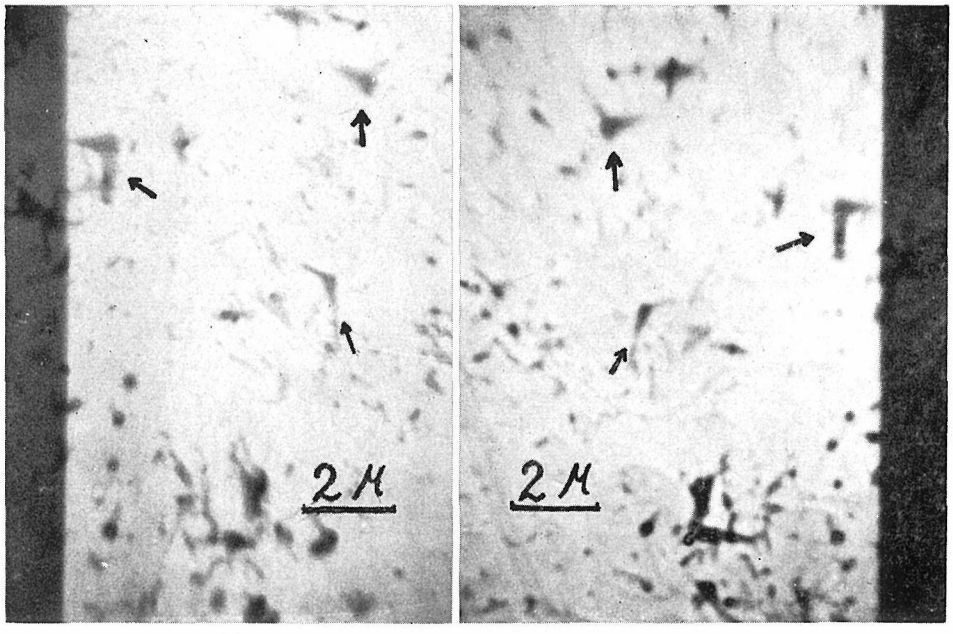

(a) (b)

Fig. 2. Electron microscopic images of MoS_2 film of 3 μ thickness with ZnO smokes on the bottom surface (a) and top surface (b) taken at 250 kV.

and bottom. They are shown in Fig. 2, indicating the images of the smokes (arrow marks) on the bottom are clearer than those on the top surfaces.

Figures 3 (a) and (b) show the images of aluminum foil commercially rolled to a thickness of 15 μ and taken at 250 kV. The bright and dark parts in both figures are the images of the foil and specimen supporting grid, respectively. The case where the grid and ZnO smoke are on the bottom surface of the foil is shown in Fig. 3(a) and the case where the grid and smoke are on the top surface is shown in Fig. 3(b). The edge of the grid can be seen much more clearly in Fig. 3(a) than in Fig. 3(b) though the focus was on the grid in both cases. It was observed electron microscopically by thinning down electrolytically that the foil consists of many grains of about 1μ in diameter. Electron diffraction from the 15 μ polycrystalline foil contained no detail but only a continuous background.

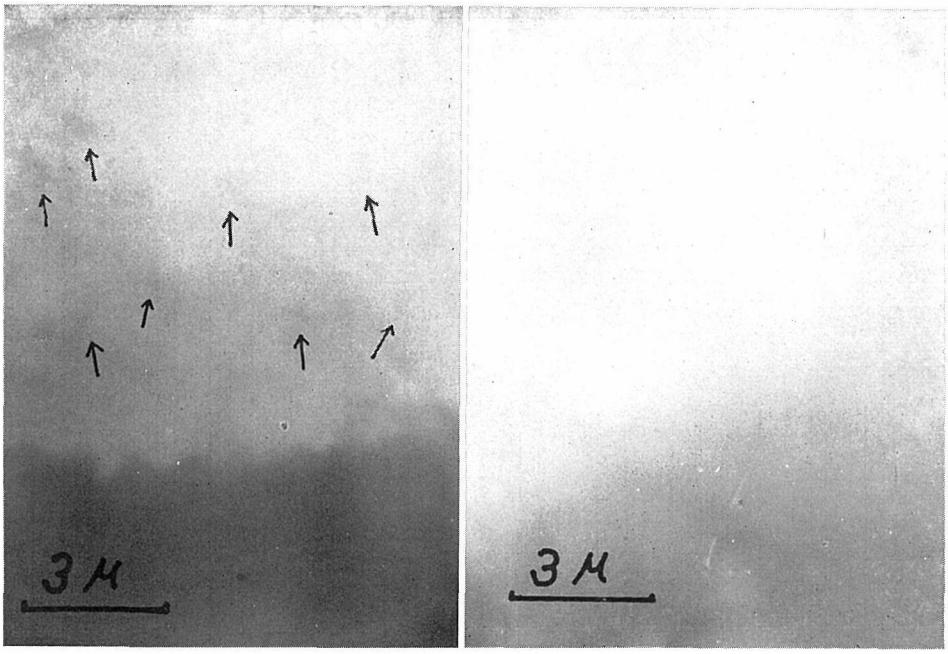

(a) (b)

Fig. 3. Electron microscopic images of Al foil commercially rolled to a thickness of 15μ. Images were taken with ZnO smokes on the bottom surface (a) and top surface (b). Arrows in (a) indicate the traces of the image of ZnO smokes. Dark parts are the images of the specimen supporting grid on the bottom surface (a) and top surface (b) of the foil.

3. ELECTRON MICROGRAPHS OF CRYSTALS TAKEN AT 300 KV

The previous discussion shows that thick crystalline specimens become more transparent at higher accelerating voltages. This is because not only the transmissive power greater but the objective aperture determined by the spherical aberration of the lens corresponds to a larger effective aperture for the scattered electrons. The maximum thickness that is transparent is the anomalous transmission regions near low index Bragg contours. However, for thick specimens the quality of the image is

reduced by chromatic aberration and divergence of electron beams as shown already. In this section some electron micrographs of metal crystals taken at 250～300 kV are illustrated and discussed.

The micrograph in Fig. 4 showing a grain boundary in stainless steel was taken at 300 kV with grain A in the Bragg angle for (111) reflection. Nine fringes are visible at the grain boundary and since they occur over about half its width, the thickness of the crystal is about 20 times the extinction distance or about 0.7 μ. Figure 5 is a picture of a stacking fault inclined to the surface of a stainless steel foil and was taken at 300 kV in the exact Bragg condition. The depth periodicity of the fringes appearing at a stacking fault[21] of a thick crystal is the same as for thickness fringes but the effect of absorption is to decrease the contrast or visibility of the fringes at the center of the stacking fault image. The number of zig-zag structures in the image of a dislocation line inclined to the film surface as shown in Fig. 6 are the same as the number of fringes in an inclined stacking fault if the film thicknesses are equal. There are about 19 zig-zag structures and the fault fringes in Figs. 5 and 6 indicating that the thickness of both films is about 0.7 μ. Figure 7 is a micrograph of a stainless steel film probably thicker than those shown in Figs. 4, 5 and 6, as no zig-zag structure can be seen in the dislocation images.

Figures 4～7 illustrate some of the characteristic features of the images of thick

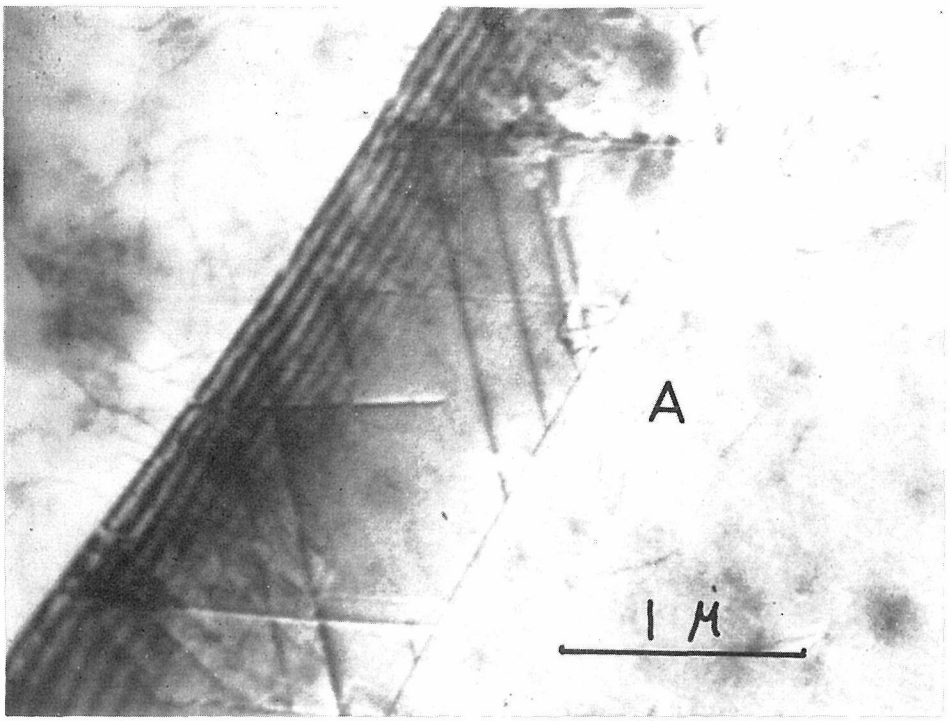

Fig. 4. An electron microscopic image of a grain boundary in stainless steel taken at 300 kV, showing the fringes appearing at one side of the image. The images of dislocations in the boundary have the characteristic contrast. Thickness of the film is known to be about 0.7 μ, from the number of the fringes.

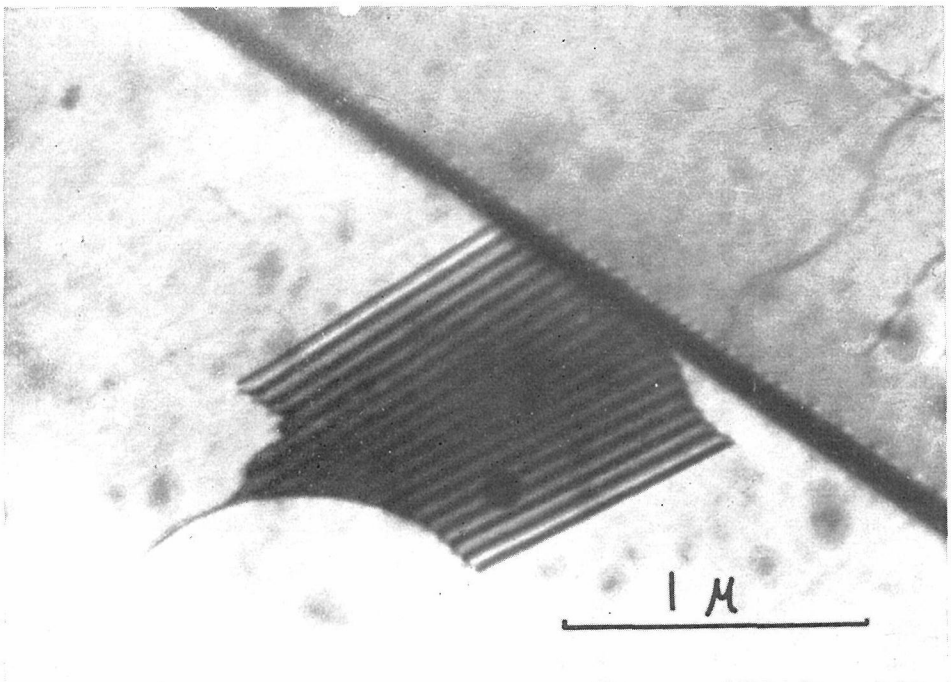

Fig. 5. An electron microscopic image of a stacking fault in stainless steel taken at 300 kV, showing the fault as a fringe system surrounded by two extended dislocations which are not straight lines. Thickness of the film is known to be about 0.7 μ from the number of the fringes.

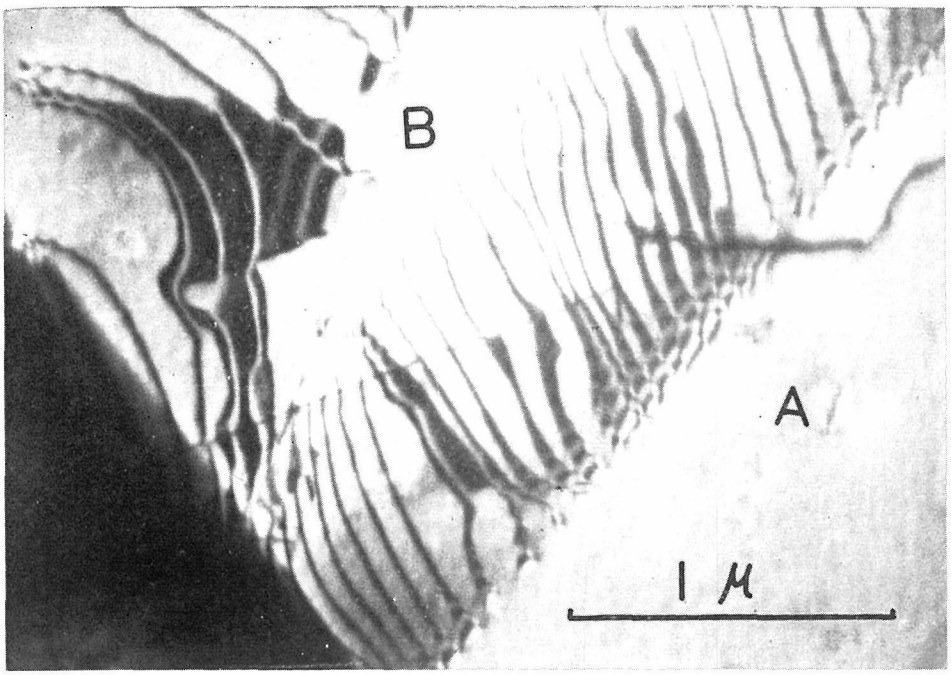

Fig. 6. An electron microscopic image of piled up dislocations in stainless steel. Note the asymmetry of the contrast of dislocation images at A and B where the dislocations meet the surfaces of the film. Dislocations are not straight lines and extend irregularly. Thickness of the film is known to be about 0.7 μ, from the number of the zig-zag structures of the images. (300 kV)

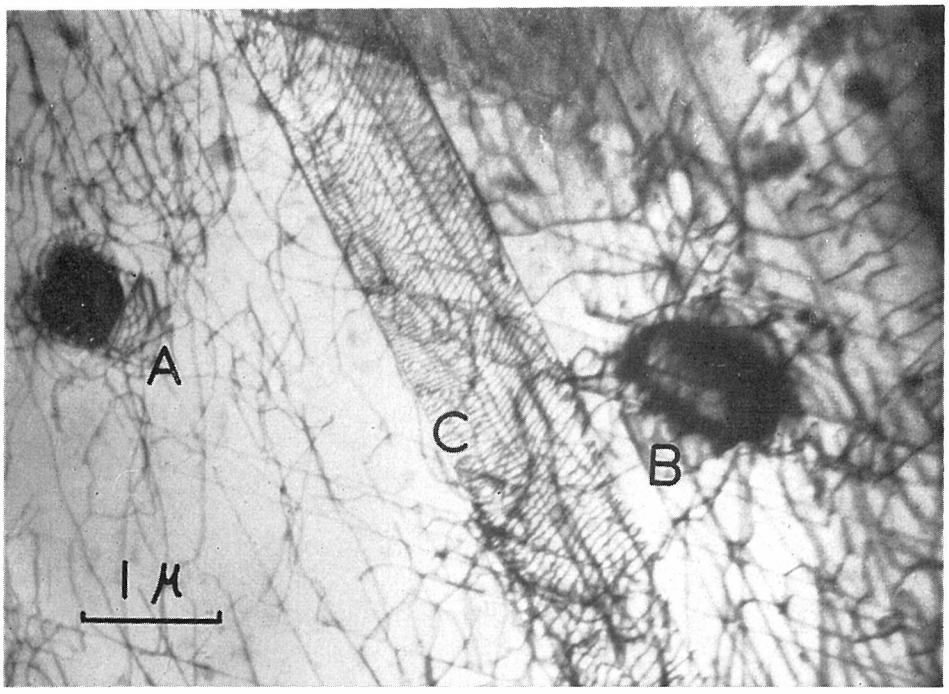

Fig. 7. Images of two grains (A and B) in crystal which are surrounded by groups of tangled dislocations and fine networks (C) of dislocations in stainless steel. (300 kV)

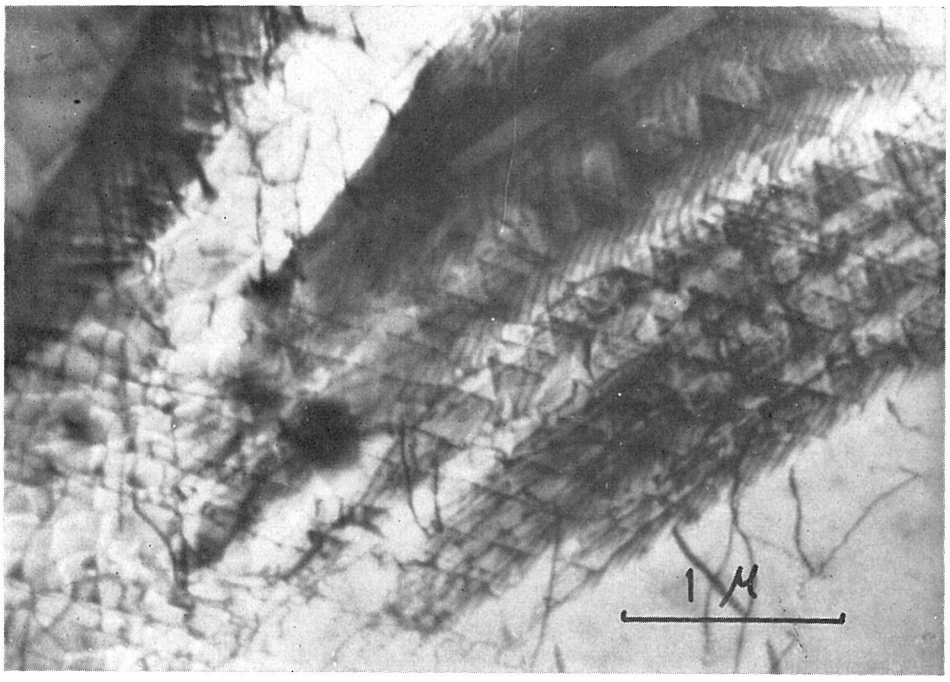

Fig. 8. An electron microscopic image of piled-up dislocation net-works in stainless steel film. Thickness of the film seems to be larger than 1 μ. (300 kV)

films differing from those of thin crystals. In Fig. 4 the thickness fringes appear only on one side of the image of the boundary and the dislocations in the boundary are observed as black or black-white straight lines and the contrast of the dislocation images decrease near the fringes. These contrast effects were not observed in the images of thin films and can be explained by anomalous absorption[24].

As detected in Fig. 5, increasing number of the fringes due to the thickning of the crystal appear only at the center of the fault which coincides with the prediction by the dynamical theory considering absorption[23].

Figures 8 and 9 are the images of stainless steel films with larger thickness than those shown in 4, 5, 6 and 7. Complicated dislocation structures are seen.

Figures 10, 11 and 12 are the images of Cu-2%Al film prepared by the electro-thinning. Figure 10 shows the dislocations in the grain boundary which appears diagonally in the middle of the figure. Figure 11 is the image of dislocations arranged nearly in parallel to each other. The thickness of this film seems to be large enough so that the dislocation arrangement in the crystal is not disturbed by the interaction with the surface. The fringes with small spacing in the center of the figure will be ascribed to the stacking fault which is formed by the extending of a dislocation. Figure 12 shows the images of a dislocation net works (right) and stacking faults (left). The thickness of the crystal is about 20 times as large as the extinction distance or about 1 μ.

Figure 13, 14 and 15 are the electron micrographs and diffraction pattern of MoS_2[22] respectively. The thickness of the specimen is 1.5 μ which is measured by a diamond tip thickness meter. The thick dark lines seem to be the images of a group of dislocation lines. The difference of the contrast on either side of the thick dislocation line indicated by A is due to the difference of orientation. Such amount of difference of orientation can not be caused only by single dislocation line. In Fig. 14, it is seen that some of the thick dark lines spread into thin dislocation lines.

Figure 16 is an image of MgO smoke crystal whose [110] is parallel to the electron beam. Even in the thickest part of the smoke, whose thickness is estimated to be 2.5 μ, some contrast can be seen.

After heating commercially rolled aluminum foil of 10 μ thickness in a vacuum of 10^{-4} mm Hg at 500°C for about 5h, the foil was electrolytically polished slightly to remove the oxide layer on the surface. The foil was cut into 2 mm $\times$ 2 mm pieces and the thickness as measured by a micrometer was found to be 8 μ. An example of an electronmicrographs taken at 250 kV is shown in Fig. 17(a) and some contrast due to inclusions, dislocation networks and grain boundaries can be seen. The white spots were usually observed only in thick films and this origin is not yet clear. The electron diffraction pattern is presented in Fig. 17(b), and only Kikuchi band and lines are visible. The images of the objective aperture used in the present observation are also recorded in Fig. 17(b).

An annealed aluminium single crystal was electropolished to be lens-shaped in cross section with the thickest part about 10μ as measured by micrometer. The 300-kV electron microscopic image shown in Fig. 18(a) was taken near the edge of the film and in Fig. 18(b) from what seemed to be the thickest part of the film with the crystal set at the Bragg angle for (111) reflection. In this case, a white band due to anomalous

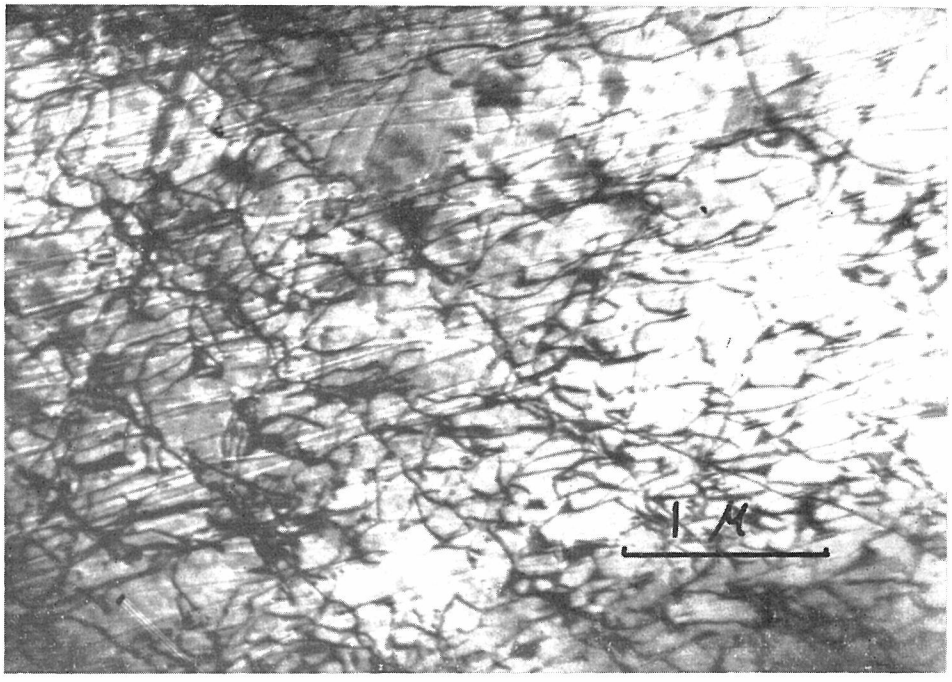

Fig. 9. An electron microscopic image of piled-up dislocations in stainless steel film. The film seems to be thicker than 1 μ. (300 kV)

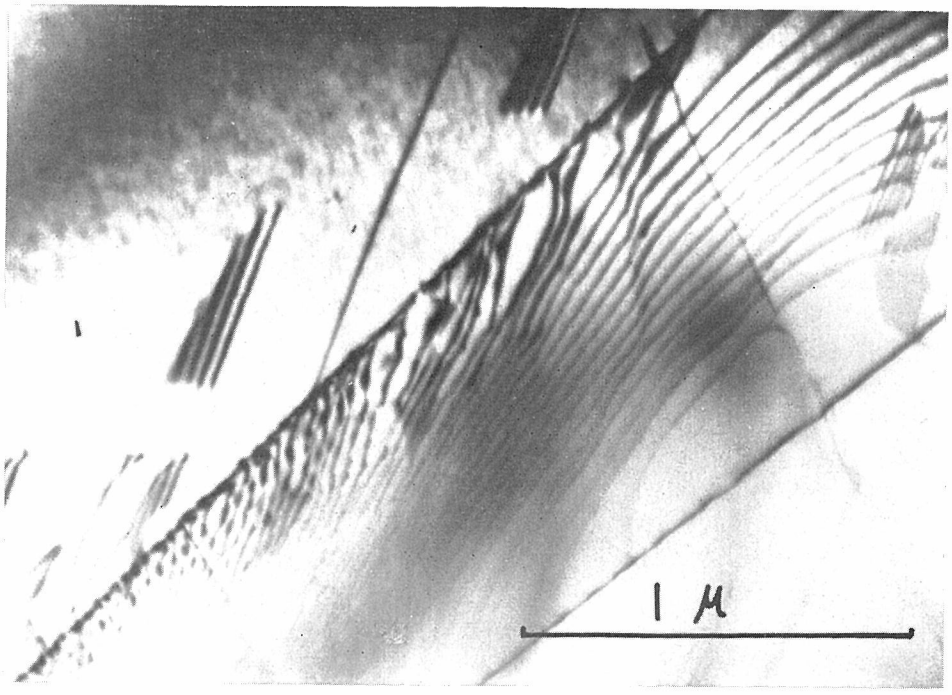

Fig. 10. An electron microscopic image of Cu-2%Al film showing dislocations in a grain boundary. The thickness of the crystal is about 1.3 μ estimated from the number of the zig-zag structures of the dislocations. (300 kV)

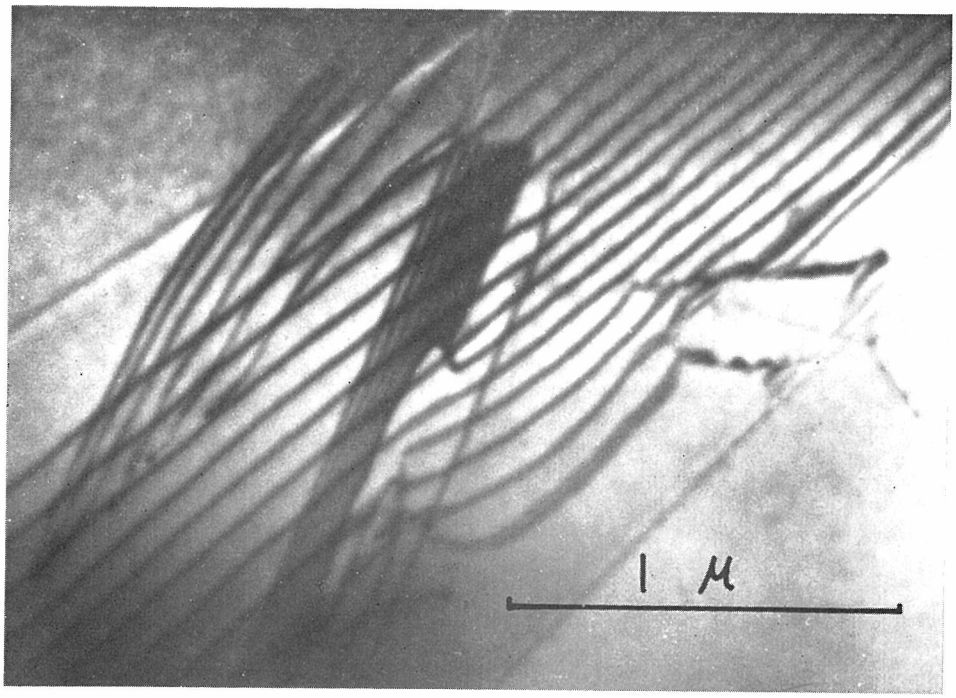

Fig. 11. An electron microscopic image of Cu-2%Al film with several dislocations in nearly parallel arrangement. A fringe system at the center of the figure is due to a stacking fault.

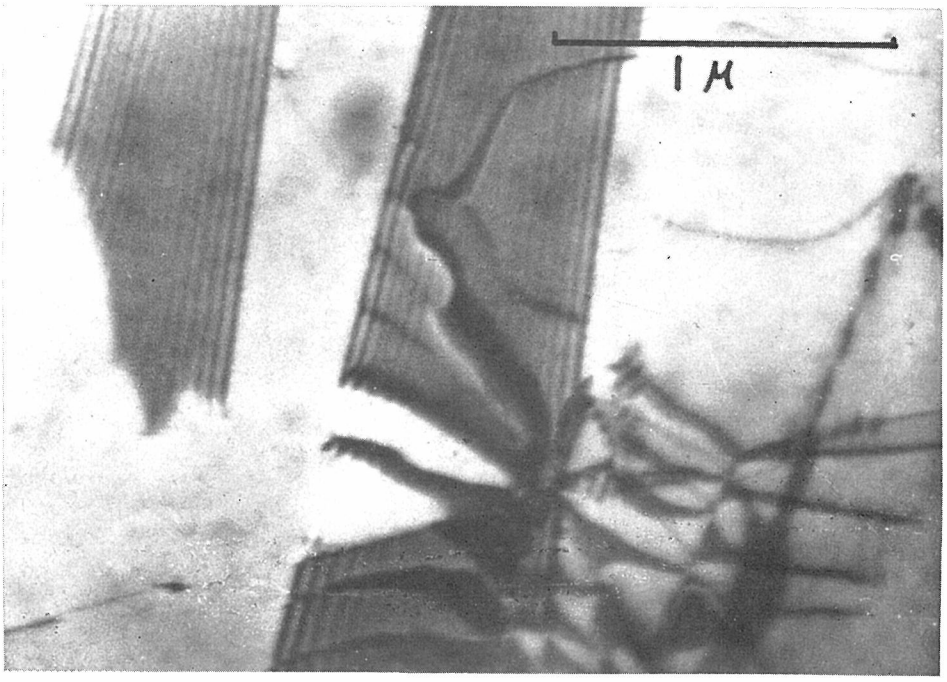

Fig. 12. An electron micrograph of Cu-2%Al film, with dislocation networks and stacking faults. The thickness of the crystal is measured to be about 1 μ from the number of stacking fault fringes. (300 kV)

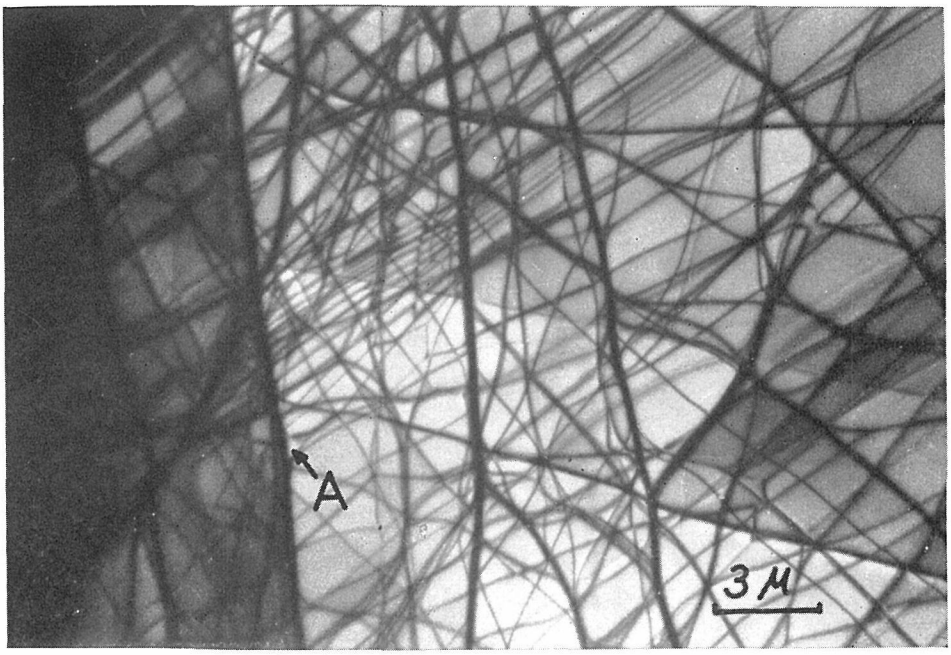

Fig. 13. An electron micrograph of MoS_2 film with thickness 1.5 μ. Each dark thick lines, one of which is indicated by A, seems to correspond to a group of dislocation lines and on either side of the dislocation, the crystal is in different orientation. (300kV)

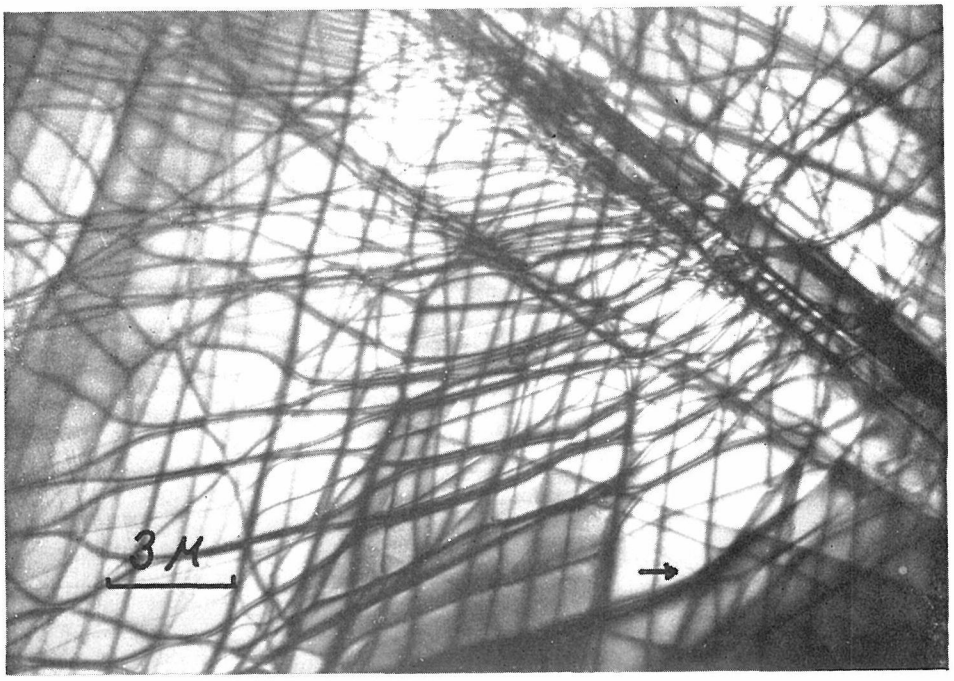

Fig. 14. An election micrograph of the same specimen shown in Fig. 13. Some of the thick dark lines spread into thin dislocation lines (arrow mark). Complicated interaction of dislocation can be seen. (300 kV)

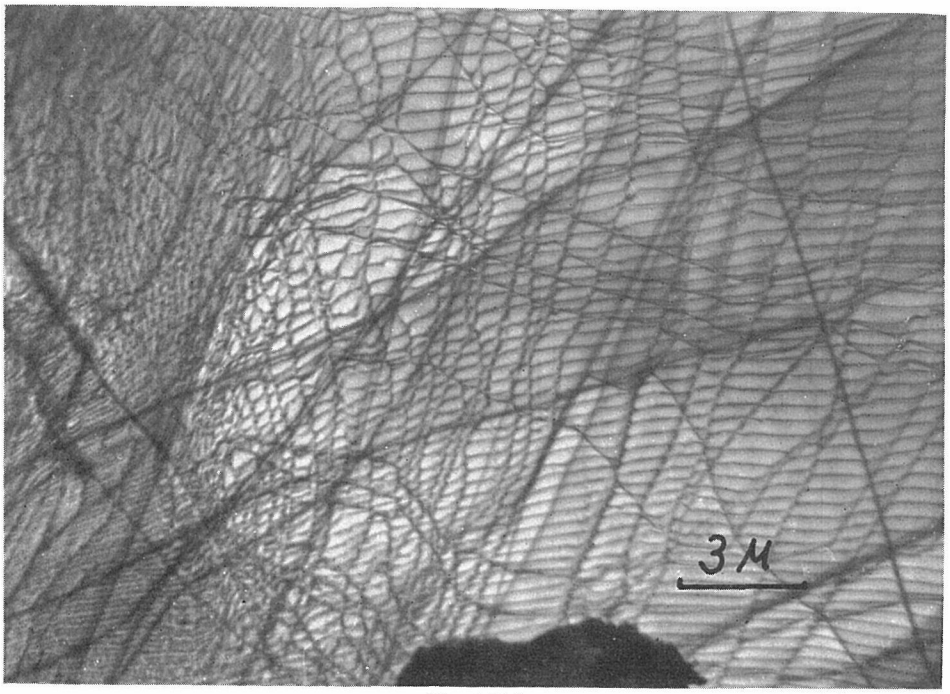

Fig. 15(a)

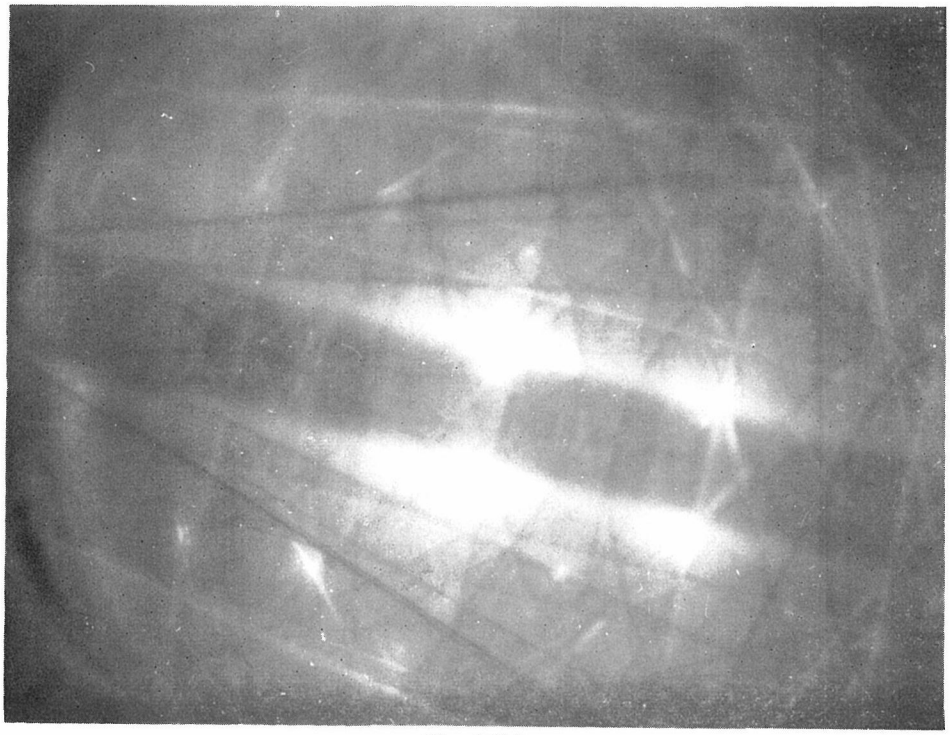

Fig. 15(b)

Fig. 15. (a) An electron micrograph of the same specimen shown in Fig. 13 showing fine dislocation networks and (b) corresponding diffraction pattern showing Kikuchi pattern.

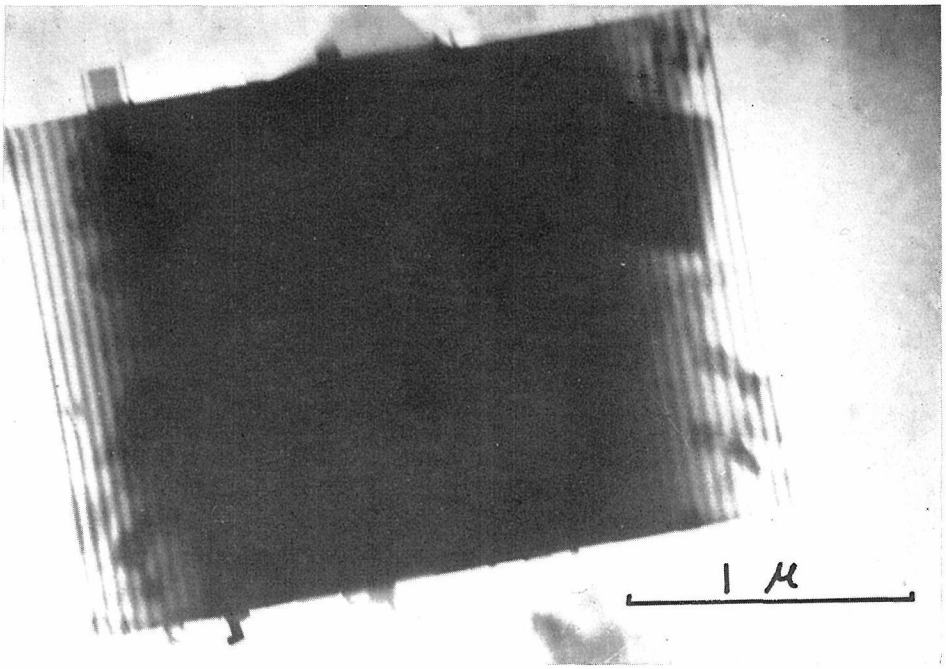

Fig. 16. An electron micrograph of MgO smoke crystal whose [110] is parallel to the incident beam. In the middle of the crystal, which is the thicknest part of the crystal (2.5 μ) some contrast can be seen. (300 kV)

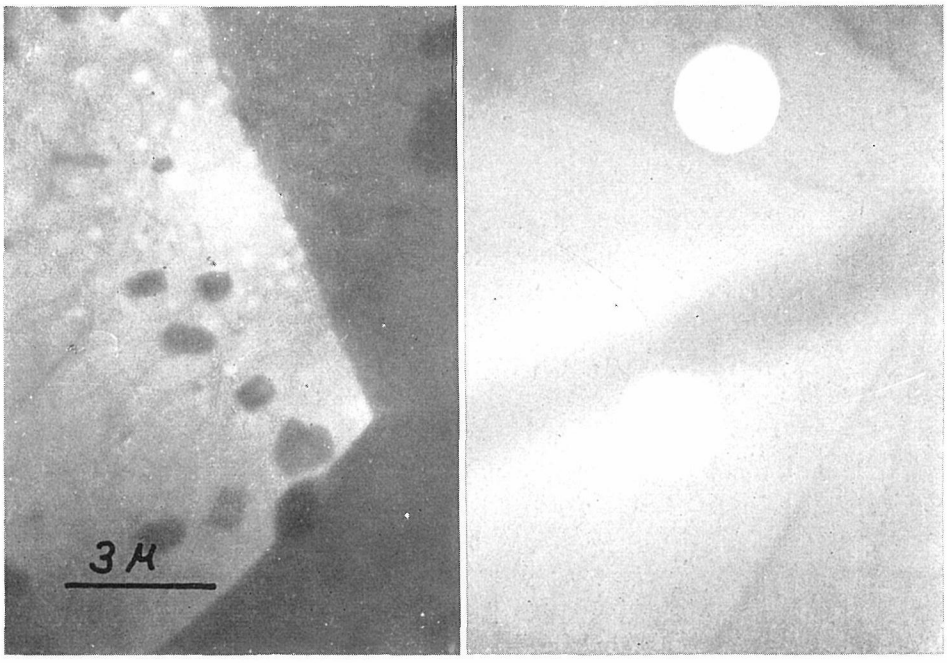

(a) (b)

Fig. 17. (a) is an electron microscopic image of aluminum foil of 8 μ thickness. (b) is a diffraction pattern from a single drystal in (a). White circular regions are the images of objective aperture used for taking the image (a). (250 kV)

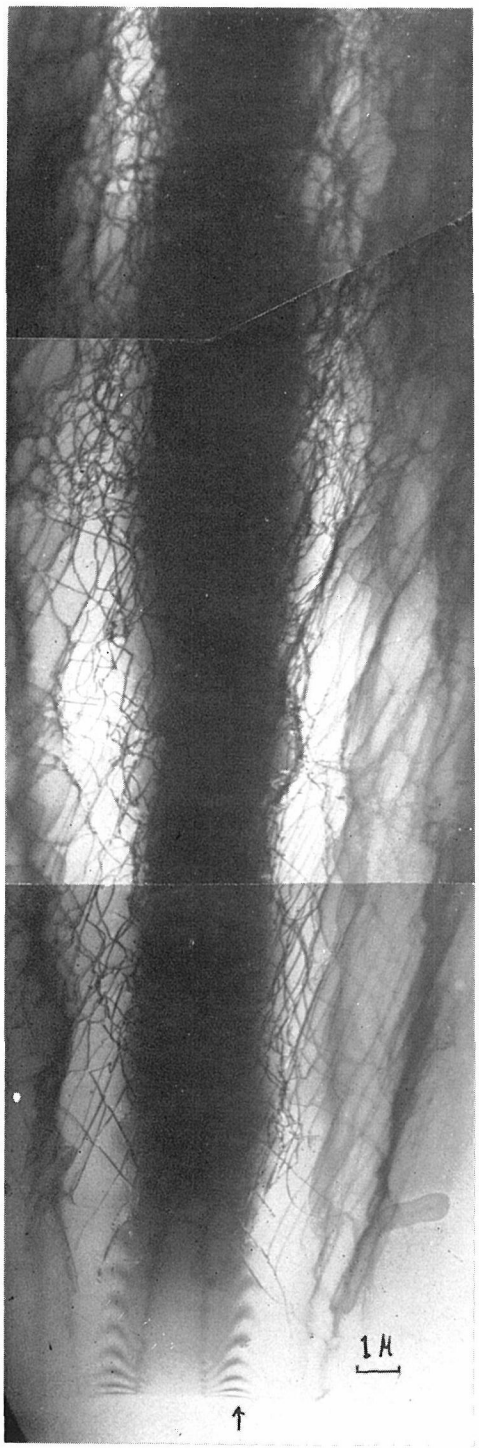

(a)

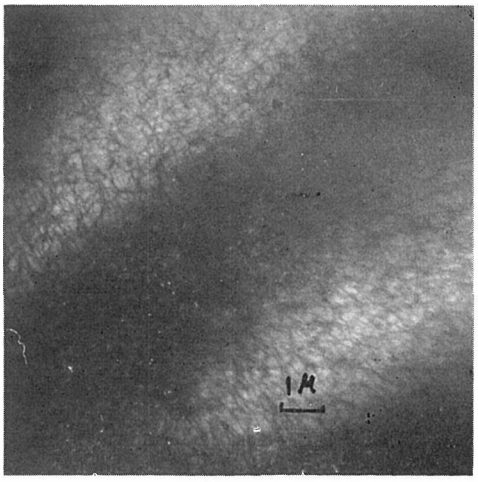

(b)

Fig. 18. Electron microscopic images of electropolished aluminum single cystal taken at 300 kV. (a) is the picture taken near the edge of the crystal. Thickness contour fringes appear near the edge at the lower part of the picture. (b) is the picture of the crystal at a thickness of about 10 μ.

transmission of electrons passed across the middle part of the film and both ends of the band terminated at the thin opposite edges as shown in the figures. As can be seen in Fig. 18(b), dislocations are visible in the film even though the thickness is about 10 μ. As has been calculated by Hashimoto[18], the equivalent thickness of polycrystalline aluminium which transmits the same intensity as a single crystal of 10 μ thickness in the exact Bragg angle is 2.9 μ.

It must be noted that if the crystal contains many dislocations the electrons are scattered by the distorted regions around the dislocations and it is very difficult to look inside the crystal clearly. In Fig. 18(b), where the thickness of the film is about 10 μ, the number of dislocations which cross a line of equivalent length 1 μ in the electron micrograph is about 30. In Fig. 18(a) where the thickness contour fringes almost disappear (thickness 6600 Å) the corresponding dislocation unit is 1.5 and at the thickness of 4 extinction distances (3320 Å) is almost zero, converting these figures to dislocation densities 30×10^7, 22×10^7, and 0 at the thicknesses of 10 μ, 6600 Å, and less than 3300 Å. This suggests that the dislocation density observed in a thin film is different from that in thick film especially in that the dislocations near the top surface of the thick film may not give a clear image enough to be detected as shown in Sec. 2. Therefore,the dislocation density in the 10 μ film is probably larger than the observed value.

4. SUMMARY OF CONCLUSIONS

1. The resolution of images of thick films is different from that of thin films. It is probable that the structures near the top surface of thick film may not be observed whereas those near the bottom surface can be seen in the observation at very high voltage.

2. Electron micrographs of Al foils of several microns and stainless steel foils of several thousand angstroms in thickness which were taken at 250～300 kV demonstrate some of the image effects due to absorption of electrons and due to geometrical configurations of the imperfections in thick crystals.

ACKNOWLEDGEMENTS

The authors' thanks are due to Professor R. Uyeda, Nagoya University, for providing the specimen shown in Figs. 2, 13, 14 and 15. The authors are grateful to Dr. T. Naiki, and Messers K. Marukawa and K. Fujita, for their assistance for the preparations of some of the specimens and to Messers M. Iwanaga and M. Ohara for the electron microscopy.

The financial support is due to the Japanese Ministry of Education.

REFERENCES

(1) H.O.Müller and E.Ruska, *Kolloid Z.*, **95,** 21 (1941).
(2) von Ardenne, *Z. Physik*, **117,** 657 (1941).
(3) V.K.Zworykin, J.Hillier, and A.W.Vance, *J. Appl. Phys.*, **12,** 738 (1941).
(4) A.C.van Dorsten, W.J.Oosterkamp, and J.B.Le Poole, *Phillips Tech. Rev.* **9,** 193 (1947).
(5) J.H.Coupland, "Proc. Intern. Conf. Electron Microscopy," London, 1954.
(6) S. Shimadzu, K.Kobayashi, and T.Hori, Report to the Special Committee for High Voltage Electron Microscopy (1951).

(7) B.Tadano, S.Katagiri, K.Ichige, Y.Sakaki, and S.Maruse, *Electron-Microscopy* (Tokyo) **7,** 7 (1959).
(8) H.M.Popov, *Izv. Akad. Nauk USSR,* **23,** 436 (1959).
(9) G.Dupouy, F.Perrier, and R. Fabre, *Compt. Rend.,* **252,** 627 (1961).
(10) K.Kohra and H.Watanabe, *J. Phys. Soc. Japan,* **16,** 580 (1961).
(11) H.Hashimoto, K.Tanaka, K.Kobayashi, E.Suito, S.Shimadzu, and M.Iwanaga, *J. Phys. Soc. Japan,* **17,** Suppl. B-II, 170 (1962); H.Hashimoto, *J. Appl. Phys.,* **35,** 277 (1964).
(12) K. Kobayashi, H. Hashimoto, E.Suito, S. Shimadzu, and M. Iwanaga, *Japanese J. Appl. Phys.,* **2,** 47 (1963).
(13) H. Hashimoto, Electron Microscopy, 5th International Congress for Electron Microscopy, Philadelphia (1962) B-II.
(14) H.Yoshioka, *J. Phys. Soc. Japan,* **12,** 618 (1957); P.B.Hirsch, *J. Phys. Soc. Japan,* **17,** Suppl. B-II 643 (1962).
(15) G.Dupouy, F.Perrier, R.Uyeda, R.Ayroles et A.Mazel, "Proc. of the Third Regional Conference," Prague, 105 (1964).
(16) G. Dupouy, F. Perrier, R. Uyeda, R. Ayroles et A. Bousquet, *C.R.Acad. Sci,* **257,** 1511 (1963).
(17) G.Dupouy and F.Perrier, *Journal de Microscopie,* **3,** 233 (1964).
(18) H.Hashimoto, *J. Appl. Phys.,* **35,** 277 (1964).
(19) H.Watanabe, *J. Phys. Soc. Japan,* **10,** 908 (1955).
(20) M.v.Ardenne, *Z. Physik,* **108,** 338 (1938).
(21) V.K.Zworykin, G.A.Morton, E.G.Ramberg, J.Hilber and A.W.Vance, "Electron Optics and the Electron Microscope", John Wiley & Sons Inc. 720p. (1948).
(22) This specimen was provided by Professor R.Uyeda with the measured value of the thickness.
(23) H.Hashimoto, A.Howie and M.J.Whelan, *Proc. Roy. Soc.* (London) **A 269,** 80 (1962).
(24) H.Hashimoto, *Metal Physics* (in Japanese) **7,** 206 (1961).